

## Output voltage ripple reduction of a high power factor mode operated isolated charge-pump AC/DC converter

Mika Sippola

Schaffner electroferrum oy, Finland  
msippola@schaffner.com

**Abstract:** This paper deals with voltage ripple reduction for a new ac/dc-converter topology based on a half-bridge driven transformer isolated charge pump. The double line output voltage ripple related to high power factor operated resonant ac/dc converters is reduced by variation of the switching frequency controlled by instantaneous line voltage feed forward. The line current waveform and electromagnetic interference are considered as well.

### 1. Introduction

The regulatory limits on line current harmonics (EN61000-3-2) have motivated work on AC/DC converters with power factor correction (PFC). In particular single-stage converters with PFC have been studied in order to reduce cost and complexity of two stage solutions (boost pre-regulator + isolated DC/DC stage) ([1], [2], [3], [4]). Often these are based on the PFC implemented with an inductor connected between line voltage and further power processing stages such as switches and transformers, and on the use of line frequency ripple energy storage capacitor. The input inductor is often used in discontinuous mode (DCM) to achieve PFC without the need to measure instantaneous line voltage and inductor current. However, it has been noted in practice that the topologies, which try to do everything in a single stage, may become quite complex and inefficient. Looking at the cost per watt their advantages over two-stage approaches become marginal [5]. An alternative, cost per watt driven solution might be based on resonant AC/DC converters with inherently sinusoidal input current characteristics but with the major drawback of the need for a relatively large output capacitor to reduce low frequency output voltage ripple [6]. Further, in [7] an AC/DC converter with the input current shaper inductance integrated into the isolation transformer (leakage inductance) and operated with secondary side charge pump capacitor was presented. Like resonant converter this has inherently high power factor but also a considerable low frequency output voltage ripple. In [7] only a simple, constant switching frequency control was used in order to minimize the complexity of the circuitry. In this paper a method to reduce output voltage ripple is presented.

### 2. Isolated charge pump AC/DC converter

The proposed converter topology is shown in figure 1. Mains voltage  $V_{ac}$  is rectified by a diode bridge and chopped across the transformer primary by a half bridge  $M_1, M_2$ . During the first half of switching period ( $M_1$  conducting) the charge pump capacitor  $C_p$  is charged towards instantaneous value of rectified line voltage ( $\frac{1}{2} V_{ac}$ ) divided by transformer turns ratio ( $N_2/N_1$ ). However, because the increase of charging current magnitude is limited by transformer leakage inductance and because of the large capacitance value of the charge pump capacitor  $C_p$  the voltage across it stays approximately constant during the charging period. During the other half of switching period ( $M_2$  conducting) some charge from pump capacitor  $C_p$  is discharged to output capacitor  $C_o$  through the output inductor  $L_o$ .

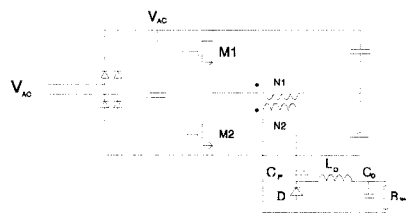


Figure 1: Converter schematic

The operation was analyzed in more detail in [7]. Here it is noted that the derivative of input current  $i_{vin}$  versus input voltage  $V_{in}$  can be shown to be:

$$\frac{\partial i_{vin}}{\partial V_{in}} = \frac{(L_s + L_o) + L_s}{8f_s(L_s + L_o)L_s} \quad (1)$$

where  $L_s$  is isolation transformer leakage inductance  
 $L_o$  is output inductance  
 $f_s$  is switching frequency

From (1) it can be concluded: 1) When switching frequency  $f_s$  is constant during the line period Eq. (1) is also constant and the input current shape follows the shape of input voltage, 2) Input current magnitude can be controlled by switching frequency  $f_s$ . This can be utilized for controlling the output voltage with the switching frequency  $f_s$ . It should be noted that the increasing

### 3D3-3

switching frequency reduces output voltage and vice versa. On the other hand the charge pump rectifier can deliver energy to the output capacitor only during the line cycle i.e. the line current waveform is cross-over distorted (the conduction angle  $\alpha < 360^\circ$ ) (Figure 2). The limited conduction angle not only causes crossover distortion to input current but also a mains frequency ripple to the output voltage and a relatively large  $C_o$  is needed to keep this at an acceptable level.

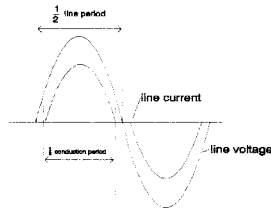


Figure 2: Line voltage and line current

#### 3. Output voltage ripple reduction

Output voltage ripple reduction based on the switching frequency modulation was chosen instead of for example pulse width modulation (PWM). After some trials a very simple concept based on input voltage feed forward was selected (Figure 3). The average output voltage is adjusted by a PI-regulator, which is controlling the inverter switching frequency with VCO. Instantaneous mains voltage is then summed into the PI-output voltage to provide the mains voltage feed forward. As a result the converter current throughput is reduced at the peak mains voltage. Similarly, the current throughput is increased at the lower mains voltage and the power throughput is constant as will be the output voltage. Thus, the line frequency output voltage ripple is reduced. Of course, by doing this the input current shape is also affected as will be seen from the measurements.

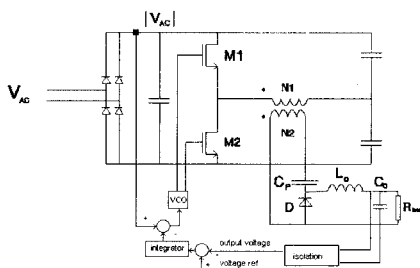


Figure 3: Control block diagram

#### 4. Prototype converter

A Prototype converter with component values in Table I was built into 2-sided FR4 PCB boards (Figure

4). The nominal switching frequency of the prototype converter was set to 240 kHz and the maximum switching frequency during peak mains voltage to 400 kHz. DC output voltage was adjusted to 10V. The switching frequency was generated using a GW INSTEK GFG-8215A function generator with VCF (frequency control voltage) – input connected to rectified mains voltage through voltage divider network.

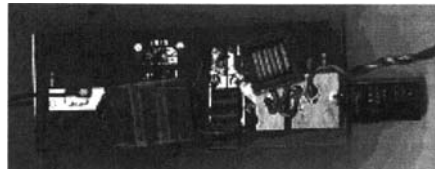


Figure 4: Prototype converter

#### 5. Measurements

The converter prototype was fed from mains through a variac in order to provide soft-start and to adjust mains voltage level. The converter was loaded with a 20W resistive load. Output voltage and input current waveforms and conducted EMI were measured using a LeCroy LT264 digital oscilloscope and an R&S ESHS 30 EMI receiver with an ESH 2-Z5 LISN. Measurements were conducted both with and without output voltage ripple reduction, and also with and without switching frequency variation.

##### 5.1 Low frequency output voltage ripple

The low frequency output voltage ripple results are shown in figure 5. In the latter case the rms value of this double line frequency voltage perturbation has been reduced as discussed in Chapter III. The reduction from 1.4V to 0.3V corresponds to reduction to 21% and after reduction the ripple is only 3% of DC voltage level (10V). In both cases there was a significant switching frequency voltage ripple at the converter output that should be further filtered by for example by using a lower effective series resistance (ESR) – filter capacitor.

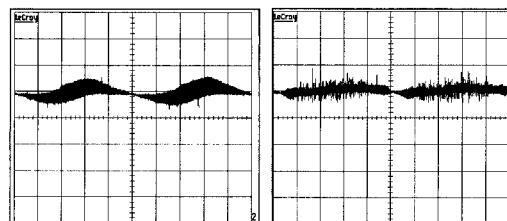


Figure 5: Output voltage ripple without (left) and with (right) switching frequency variation (2V/div : 2ms/div)

### 5.2 Input current waveform

The input current measurement results are shown in figure 6. As required for output voltage ripple reduction the switching frequency variation has increased the input current at low input voltage levels and reduced it at the mains voltage peak values. This corresponds to constant input power as required by constant output power and output voltage as well. On the other hand without switching frequency variation the converter shows more or less linear voltage-current-characteristics according to Eq.1. and Fig.2.

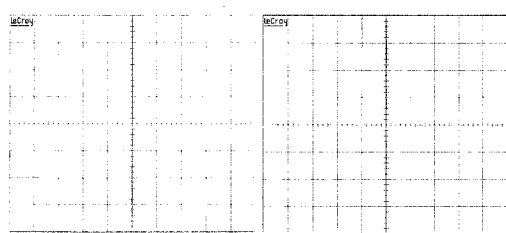


Figure 6: Input current without (left) and with (right) switching frequency variation

### 5.3 Conducted EMI

The conducted EMI measurement results of the test converter are shown in figure 7. Both peak (higher curve) and average (lower curve) measurements are displayed. 20ms measurement time and 10 kHz IF bandwidth were used. General envelope of the emission spectrum has remained the same but some interesting observations can be made. 1) Without switching frequency variation the discrete harmonics of switching frequency are clearly visible 2) At higher frequencies interference is typically of common mode type the switching frequency variation results in approx. 10 dB higher peak emission. This is obviously due to fact that the increase of switching frequency also increases the energy associated with capacitively coupled displacement (i.e. common mode) currents as well.

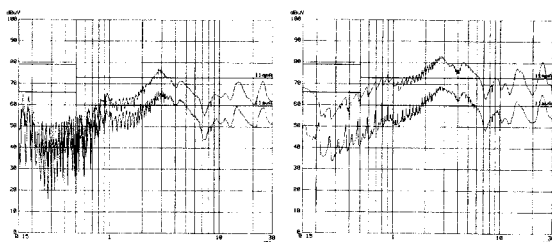


Figure 7: Conducted EMI without (left) and with (right) switching frequency variation

3) At the low frequency range where emission is typically differential mode the switching frequency variation has reduced the average switching frequency harmonic components about 15dB. Because it is often just the

average low frequency differential emissions, such as the switching frequency and the first harmonics that require most bulky filtering this can be considered as a particularly interesting result.

### 6. Summary and conclusion

In this work a new AC/DC converter topology was presented, analyzed and verified with measurements. The converter features are summarized in table 1.

Table 1: AC/DC-converter features

| Feature            | Comment   |
|--------------------|---|
| Output voltage     | 6% low frequency ripple                             |
| Galvanic isolation | OK  |
| Power factor       | 94% (OK)  |
| EMI                | Continuous output current, low ripple input current |
| Efficiency         | 83%   |
| Inrush current     | not considered, approx. 300 nF primary capacitance  |
| Size               | not considered                                      |
| Cost               | not considered                                      |

The inherently sinusoidal input current characteristics of half-bridge driven charge pump rectifier and other desired features such as zero voltage switching, acceptable efficiency and low component count makes this topology suitable for low cost per watt / high power density AC/DC converters. Potential applications of the converter are: low cost on board PFC AC/DC converters of AC-distributed power systems, 12V halogen lamp power supplies, battery chargers and portable AC/DC converters.

In order to quantify the benefits of the new converter topology the volume and cost of power components required by different rectifier alternatives (Fig 9.1 – 9.4) are compared.

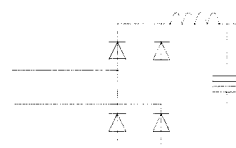


Figure 8: Passive PFC (Type 1)

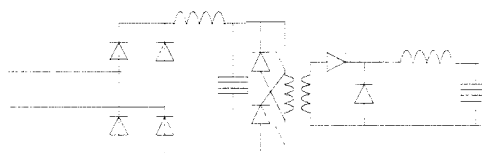


Figure 9: Passive PFC and Forward DC/DC (Type 2)

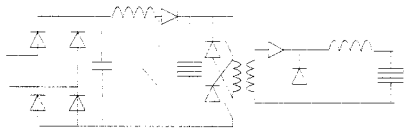


Figure 10: Boost PFC and Forward DC/DC (Type 3)

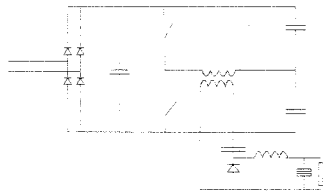


Figure 11: Proposed converter (Type 4)

Component costs (Table 9.1) are taken from ELFA and Farnell catalogues. It should be noted that for mass manufacturing an order of magnitude lower absolute component costs may be possible. Proposed converter has isolation transformer and output inductor integrated into same E32 core. Other converters use EFD20 cores for transformers and high frequency inductors.

Table 2: Component cost calculation.

| Component                  | Cost  | Type 1 | Type 2 | Type 3 | Type 4 |       |       |       |      |
|----------------------------|-------|--------|--------|--------|--------|-------|-------|-------|------|
| MOSFET IRF830              | 11.53 | 0      | 0.2    | 23.06  | 3      | 34.59 | 2     | 23.06 |      |
| Rect Diode 1N4007          | 1.52  | 4      | 6.08   | 4      | 6.08   | 4     | 6.08  | 4     | 6.08 |
| Fast Rec. Diode BY299      | 5.05  | 0      | 0.2    | 10.10  | 3      | 15.15 | 0     | 0     |      |
| Schottky diode             | 5.00  | 0      | 0.2    | 10.00  | 2      | 10.00 | 1     | 5.00  |      |
| Planar F-core E32 3F4      | 10.55 | 0      | 0      | 0      | 0      | 0     | 1     | 10.55 |      |
| Planar I-plate E32 3F4     | 9.28  | 0      | 0      | 0      | 0      | 0     | 1     | 9.28  |      |
| Coil former EFD20          | 10.50 | 0      | 0.2    | 21.00  | 3      | 31.50 | 0     | 0     |      |
| ferrite core half EFD20    | 8.29  | 0      | 0.4    | 33.16  | 6      | 49.74 | 0     | 0     |      |
| ELKO 10µF 450V             | 13.78 | 1      | 13.78  | 1      | 13.78  | 1     | 13.78 | 0     | 0    |
| ELKO 2200µF 16V            | 4.56  | 0      | 0.1    | 4.56   | 1      | 4.56  | 0     | 0     |      |
| ELKO 2200µF 16V            | 28.82 | 0      | 0      | 0      | 0      | 0     | 1     | 28.82 |      |
| X2 cap CAP MKT 0.1µF 400V  | 2.15  | 0      | 0.1    | 2.15   | 1      | 2.15  | 2     | 4.30  |      |
| Choke 51 mH 1.4A peak T200 | 29.00 | 1      | 29.00  | 1      | 29.00  | 0     | 0     | 0     |      |
| Total                      |       |        | 48.86  | 152.89 | 167.55 |       |       | 87.09 |      |

The results (Figure 9.5) show that the passive solution has the lowest cost. However, it does not provide galvanic isolation and the output voltage is approximately the peak value of line voltage and cannot be adjusted. The size of the required passive choke may also be quite bulky. The additional forward stage for output voltage regulation triples the component costs. Size reduction by active PFC may be required for miniaturization. However, this solution has the highest costs (3.4 times passive). The component costs of the proposed converter are approximately in half way between other solutions.

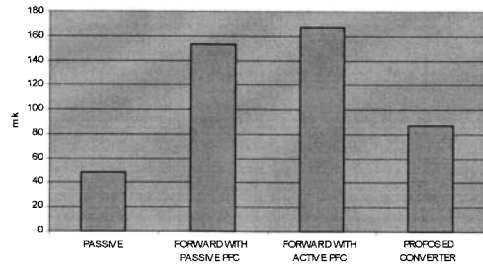


Figure 12: Power component cost comparison

The volume of passive PFC solutions is dominated by the bulky PFC choke. Forward with active PFC has the smallest volume. The proposed converter has only 13% higher volume than forward with active PFC with the size being dominated by the bulky output electrolytic capacitor.

Passive PFC may be preferred for lowest cost and highest reliability in applications where size and weight are not critical such as industrial motor drives or PC's and other office equipment. Smallest volume and best performance of active PFC may be preferred in telecom systems where costs are not absolutely critical. Proposed converter may have applications in cost critical small volume applications such as laptop AC/DC supplies, consumer electronics and 12V halogen lamp power supplies as already discussed.

The further work on this subject includes design optimization of proposed converter for various applications. Efficiency, thermal design, EMC and other practical aspects must also be addressed.

7. References

- [1] Chongming Q., Smedley, K.M., "A topology survey of single-stage power factor corrector with a boost type input-current-shaper", *Proceedings of 15th IEEE Applied Power Electronics Conference and Exposition 2000*, vol.1, p. 460 – 467, 2000
- [2] Kheraluwala, M.H.; Steigerwald, R.L.; Gurumoorthy, R. "A fast-response high power factor converter with a single power stage", *Proceedings of 22nd IEEE Power Electronics Specialists Conference*, p. 769 – 779, 1991
- [3] Madigan, M.; Erickson, R.; Ismail, E. "Integrated high quality rectifier-regulator", *Proceedings of 23rd IEEE Power Electronics Specialists Conference*, vol. 2, p.1043-51, 1992
- [4] Redl, R.; Balogh, L.; Sokal, N.O. "A New family of single-stage isolated power-factor correctors with fast regulation of the output voltage", *Proceedings of 25th IEEE Power Electronics Specialists Conference*, vol. 2, p. 1137 – 1144
- [5] Sharifipour B., Huang J.S., Liao P., Huber L., Jovanovic M.M., "Manufacturing and cost analysis of power-factor-correction circuits", *Proceedings of 13th IEEE Applied Power Electronics Conference*, vol.1, p.490-494, 1998
- [6] Schutten M.J., Steigerwald R.L., Kheraluwala M.H., "Characteristics of Load Resonant Converters Operated in a High Power Factor Mode", *Proceedings of 6th IEEE Applied Power Electronics Conference*, pp. 5 – 16, 1991
- [7] Sippola M., Sepponen R., "A new AC/DC converter topology with high power factor", *International Journal of Electronics*,